Avalanche instability as nonequilibrium quantum criticality

Xi Chen and Jong E. Han*
Department of Physics, State University of New York at Buffalo, Buffalo, New York 14260, USA

(Received 14 July 2023; revised 2 January 2024; accepted 29 January 2024; published 20 February 2024)

A fundamental instability in the nonequilibrium conduction band under an electric field bias is proposed via the spontaneous emission of coherent phonons. Analytic theory, supported by numerical calculations, establishes that the quantum avalanche, an abrupt nonequilibrium occupation of excited bands, results from the competition between the collapse of the band minimum via the phonon emission and the dephasing of the electron with the environment. The continuous avalanche transition is a quantum phase transition with the nonequilibrium phase diagram determined by the avalanche parameter β, with peculiar reentrant avalanche domes close to the phase boundary. We further confirm the nature of the quantum avalanche with the temperature dependence.

DOI: 10.1103/PhysRevB.109.054307

I. INTRODUCTION

Materials under strong electromagnetic fields have been extensively studied in the past half-century. In particular, the resistive phase transition driven by a high electric field has generated strong research efforts [1–5]. However, despite the scientific and technological importance of the phenomena, conceptual advancement has been limited since it requires an understanding of many-body dynamics far from equilibrium [6].

The challenge partly comes from the lack of theoretical milestones. Despite mounting experimental reports [5,7–10], theories have not provided decisive new insights into outstanding issues. One such problem is resistive switching, in which the mechanism of the insulator-to-metal transition by a dc electric field has been debated, as to the electronic or thermal origin, for many decades without much consensus. Part of the problem is that theoretical efforts have often been too complex to relate to well-established equilibrium counterparts systematically. The goal of our analytic theory is to identify a mechanism of nonequilibrium quantum transition akin to critical phenomena and provide a conceptual and transparent framework that could initiate future discussion.

In the past decades, we have asked how electrons overcome the energy gap to induce dielectric breakdown, mainly within the framework of Landau-Zener tunneling [1,7,11]. Despite strong efforts, theories failed to address the energy-scale discrepancy where the experimental switching fields are orders of magnitude smaller than theoretical predictions [12–15]. In a recent work [16], an alternative answer was proposed. In materials, electrical resistivity is not infinite and, with bias, there exist many charge carriers present in the bulk limit, despite with very dilute concentration. Once electrons are coupled to an inelastic medium, instability develops with a uniform electric field, in principle at infinitesimally small strength, leading to an eventual resistive breakdown of the system at experimental scales [16].

In this work, we demonstrate that the correlated resistive switching is an immediate consequence of a fundamental nonequilibrium instability of electron bands in dc nonequilibrium. Through a minimal electronic dissipation model we show that any bands are in principle subject to avalanching instability and the occurrence of the quantum-avalanche phase transition is determined by the competition with dephasing.

II. MODEL AND CRITERION OF QUANTUM AVALANCHE

We introduce a model of a one-dimensional electron gas coupled to optical phonons with electrons subject to a static and uniform electric field E with the Hamiltonian

$$H(t) = \int \left[\psi^\dagger(x)\left(\frac{1}{2m}(-i\hbar\partial_x + eEt)^2 + \Delta\right)\psi(x) + \frac{1}{2}\left[p_\varphi(x)^2 + \omega_0^2\varphi(x)^2\right] + g_{\rm ep}\varphi(x)\psi^\dagger(x)\psi(x)\right]dx, \quad (1)$$

with the (spinless) electron creation/annihilation operator $\psi^\dagger(x)/\psi(x)$, the Einstein phonon field $\varphi(x)$ of frequency ω_0 with its conjugate momentum $p_\varphi(x)$, and the electron-phonon coupling constant $g_{\rm ep}$. The conduction band is placed Δ above the Fermi energy of the particle reservoir. A uniform dc electric field is included as a vector potential $-eEt\hat{\mathbf{x}}$ in the temporal gauge [17,18]. We use the unit system that $\hbar = e = k_B = 1$, with the Boltzmann constant k_B.

The system is coupled to the environment with electrons and phonons connected to the fermionic and bosonic baths [16,19,20], respectively. The importance of phonon baths has been highlighted [16,21] recently. The fermion reservoirs account for the exchange of electrons from bands outside the model (such as substrate) and provide dissipation. More importantly, this mechanism sets the electron lifetime via dephasing from external sources other than phonons. The hybridization to the fermion bath is given as Γ, which we

*jonghan@buffalo.edu

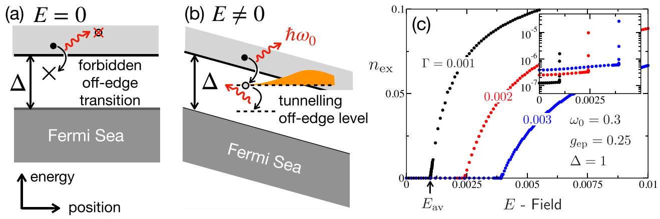

FIG. 1. (a) Energy scheme of a conduction band above the Fermi level by Δ at equilibrium. Spontaneous emission of phonons into an electronic level below the band edge is not allowed. (b) With the electric field $E > 0$, the potential slope provides energy levels tunneling below the band edge, enabling the spontaneous transition into the forbidden region by emitting local phonons. As the electronic replica state, with its energy lowered by ω_0, is reinforced by the multiple-phonon processes, an abrupt quantum transition occurs in an avalanche. (c) Numerical results showing occupation number $n_{\rm ex}$ of the conduction band as a function of E. The avalanche field $E_{\rm av}$ is an increasing function of the dephasing rate Γ, suggesting that the dephasing competes with the avalanching mechanism. Counterintuitively, smaller preavalanche occupations led to earlier avalanches, as shown in the inset.

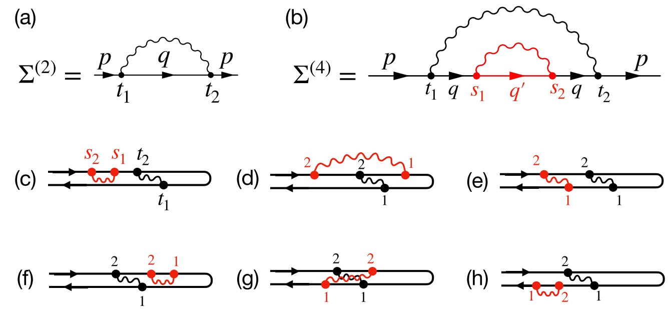

FIG. 2. (a) Lowest-order self-energy to electron by electron-phonon coupling. Electron (solid line) emits/absorbs a phonon (wiggly line) in the scattering. (b) The next-order self-energy showing two-phonon process. The integral is performed over the internal (red) Keldysh times s_1 and s_2. (c) Out of the 12 possible arrangements of (s_1, s_2) on the Keldysh contour, the dominant contribution comes with $s_{1,2} < t_{1,2}$ on each contour, as shown.

assume to be independent of energy and to be structureless with infinite bandwidth, for simplicity. The electrons can deposit their excess energy into phonons with the scattering rate controlled by the coupling constant $g_{\rm ep}$, with the excited phonons eventually decaying into an Ohmic bath [22,23].

This minimal model has been shown to induce a quantum avalanche [16] where a phase transition to a strong nonequilibrium occupation of the band occurs at a small electric field scale. The mechanism for the quantum avalanche is as follows. As depicted in Fig. 1(a), spontaneous phonon emission does not occur in the $E = 0$ limit due to the absence of states below the band minimum. Even with the faint line broadening into the gap due to Γ, these states are quite insignificant. However, with a nonzero electric field [see Fig. 1(b)], the potential slope provides electronic levels at any energy. [Here, we temporarily switch to the static gauge with potential $V(x) = -eEx$ for the sake of argument.] While the off-edge states are due to the evanescent tail centered at a different position as depicted as the orange envelope function in (b), it allows much enhanced spontaneous phonon emission compared to (a). This smear of band edge due to a uniform electric field is the Franz-Keldysh effect [24]. With the replica state generated by a phonon emission reinforces the evanescent off-edge state so that it can act as the reference state that generates the second replica state. The formation of the multiple replicas requires the phase coherence between the electron and the phonon throughout, which is limited by the electron dephasing time. This sets the threshold for the quantum avalanche. We note that the nature of the transition is spontaneous electronic transition below the band, instead of the sequential dissipation of excess electronic energy into phonon quanta.

We emphasize that fully numerical calculations confirm the following theoretical analysis. As published in several nonequilibrium dynamical mean-field theory works [16,19,25,26], the dissipation mechanisms are rigorously implemented in self-consistent calculations. It is essential to include the dissipation on an equal footing as the system Hamiltonian to ensure numerical convergence. In the lattice model, the static gauge is used to exploit the time-translation invariance of the steady state with the tight-binding parameter t set to $ta^2 = \hbar^2/(2m) = 1$ with lattice constant a set to 1. The details about the numerical method can be found in previous publications mentioned above.

Before we present the analytic theory, we discuss numerical evidence for the quantum avalanche, in Fig. 1(c). The occupation number of the band $n_{\rm ex}$ shows a continuous phase transition at the finite electric field at $E_{\rm av}$. There are two key observations: (1) the avalanche field $E_{\rm av}$ is almost linearly proportional to the coupling to the environment Γ and (2) the occupation number before the avalanche has no direct consequence on the strength of $E_{\rm av}$. The fact that $E_{\rm av} \propto \Gamma$ indicates that the avalanche arises from the formation of off-edge states established during the timescale set by the dephasing time Γ^{-1}. That is, with a long-dephasing time ($\Gamma \to 0$), the multiphonon replica becomes more robust with a smaller electric field. The second observation directly points to the quantum nature of the transition. It is highly counterintuitive that the initial occupation, which reflects the thermal occupation of the conduction band via the line broadening Γ, goes against the avalanche transition. As will be argued shortly about the gap dependence of the avalanche, the avalanche only requires the existence of the particle source, but not the proximity of the particle reservoirs. We confirmed numerically that the avalanche occurs in square and cubic lattices.

Now, we identify the condition for the abrupt increase of electron occupation in the band. The electron occupation is directly obtained from the lesser Green's function (GF), $n_{\rm ex} = -i\int G^<_p(t,t)\frac{dp}{2\pi}$, with the lesser GF defined as $G^<_p(t_2,t_1) = i\langle c^\dagger_p(t_1)c_p(t_2)\rangle$, with the Fourier transformed fermion variable $c_p = \int e^{-ipx}\psi(x)dx$. The enhancement of occupation results from the lesser self-energy $\Sigma^<$, symbolically through $G^< = G^R\Sigma^<G^A$. Figures 2(a) and 2(b) represent the two lowest-order self-energies due to one-phonon and two-phonon emission, respectively, and we look for the condition that

these processes lead to comparable magnitude so that we expect an infinite summation of these "rainbow" diagrams to lead to an occupation avalanche.

The lowest-order self-energy $\Sigma_p^{(2),<}(t_2, t_1)$, Fig. 2(a), can be written [17] as

$$\Sigma_p^{(2),<}(t_2, t_1) = i g_{\mathrm{ep}}^2 \int \frac{dq}{2\pi} D_0^<(t_2, t_1) G_{0q}^<(t_2, t_1), \tag{2}$$

where $D_0^<(t_2, t_1)$ is the standard Keldysh GF for phonon and $G_{0q}^<(t_2, t_1)$ for noninteracting electron with momentum q. The integral in the continuum model is for $q \in (-\infty, \infty)$. The electronic lesser GF is given as

$$G_{0p}^<(t_2, t_1) = i n_<(p) e^{-\Gamma|t_2 - t_1|} U_p(t_2, t_1), \tag{3}$$

with an unspecified initial occupation $n_<(p)$ and the time-evolution factor of a free electron

$$\begin{aligned} U_p(t_2, t_1) &= \exp\left[-i \int_{t_1}^{t_2} \left(\frac{(p + Es)^2}{2m} + \Delta\right) ds\right] \\ &= \exp\left[-i \left(\frac{(p + ET)^2}{2m} + \Delta\right) t - \frac{iE^2 t^3}{24m}\right], \end{aligned} \tag{4}$$

with the average time $T = \frac{1}{2}(t_2 + t_1)$ and the relative time $t = t_2 - t_1$. We note that physical observables are gauge independent [27–29] and the mechanical momentum $\bar{p} = p + ET$ appears in the manner as above. The bare phonon Green's function D_0 is defined as

$$\begin{aligned} D_0^{\gtrless}(t) &= -i \langle \varphi(\pm t) \varphi(0) \rangle \\ &= -\frac{i}{2\omega_0} \{ n_b(\omega_0) e^{\pm i\omega_0 t} + [1 + n_b(\omega_0)] e^{\mp i\omega_0 t} \}, \end{aligned} \tag{5}$$

with the Bose-Einstein function $n_b(\omega_0) = (e^{\omega_0/T} - 1)^{-1}$.

Assuming that the occupation of the conduction band is only at $\bar{p} \approx 0$ up to the onset of the avalanche and that the bath temperature T is much smaller than the phonon energy ω_0, we may write $n_<(p) \approx 2\pi n_{\mathrm{ex}} \delta(p + ET)$ such that $n_{\mathrm{ex}} = \int n_<(p)(dp/2\pi)$ with the total excitation n_{ex} and obtain

$$\Sigma_p^{(2),<}(t_2, t_1) \approx \frac{i n_{\mathrm{ex}} g_{\mathrm{ep}}^2}{2\omega_0} e^{-\Gamma|t| - i[(\Delta - \omega_0)t + E^2 t^3/24m]}. \tag{6}$$

Note that the band edge Δ is shifted down by ω_0 due to the phonon emission.

The next-order self-energy, while we only look at the nested diagram, can be quite formidable when integrated over the Keldysh times. The fourth-order self-energy $\Sigma^{(4)}(t_2, t_1)$, as depicted in Fig. 2(b), can be written as

$$\begin{aligned} \Sigma^{(4)}(t_2, t_1) = g_{\mathrm{ep}}^4 \int_K ds_1 \int_K ds_2 G(t_2, s_2) D_0(t_2, t_1) \\ \times G(s_2, s_1) D_0(s_2, s_1) G(s_1, t_1), \end{aligned} \tag{7}$$

with the internal times $s1$ and $s2$ on the Keldysh contour marked as red. Six of the twelve permutations for $s_{1,2}$ are shown in Fig. 2(b). By using the fact that $|G^<| \ll |G^>|$ in the dilute limit before the avalanche, the only dominant time ordering is as shown in (e), which is $-\infty < s_{1,2} < t_{1,2}$ in the backward/forward Keldysh time contour, respectively. For instance, with the time ordering shown in (c), not only is the Green's function product $G^>(t_2, s_2) G^<(s_2, s_1) G^<(s_1, t_1)$ in the second order of $G^<$, but also it is reducible into the self-energy of the one-particle Green's function. Therefore, in the low-density limit, the fourth-order self-energy is approximated as

$$\begin{aligned} &- i \frac{g_{\mathrm{ep}}^4}{(2\omega_0)^2} \int \frac{dq}{2\pi} \int \frac{dq'}{2\pi} \int_{t_1}^{-\infty} ds_1 \int_{-\infty}^{t_2} ds_2 n_<(q') \\ &\times e^{-\Gamma(t_2 - s_2 + t_1 - s_1 + |s_2 - s_1|)} e^{i\omega_0(s_2 - s_1 + t_2 - t_1)} \\ &\times U_q(t_2, s_2) U_{q'}(s_2, s_1) U_q(s_1, t_1). \end{aligned} \tag{8}$$

As detailed in Appendix A, $\Sigma_p^{(4),<}(t)$ is well approximated as

$$\begin{aligned} \Sigma_p^{(4),<}(t) \approx -\frac{n_{\mathrm{ex}} m g_{\mathrm{ep}}^4}{(2\omega_0)^2} e^{-i[(\Delta - 2\omega_0)t + E^2 t^3/24m]} \\ \times \int \frac{dq}{2\pi} \int ds \frac{e^{i(q^2/2m + \omega_0)s}}{qE(t + s) + 2im\Gamma}. \end{aligned} \tag{9}$$

In the above approximation, it is crucial that the dephasing rate Γ and the resulting electric field E are much smaller than other energy scales such as the phonon frequency ω_0 and the kinetic energy. We define the figure of merit value λ for the enhancement of multiphonon effect as $\Sigma_p^{(4),<}(0)/\Sigma_p^{(2),<}(0)$ and

$$\lambda \approx \frac{i m g_{\mathrm{ep}}^2}{2\omega_0} \int \frac{dq}{2\pi} \int ds \frac{e^{i(q^2/2m + \omega_0)s}}{qEs + 2im\Gamma}. \tag{10}$$

This integral is readily expressed in terms of the modified Bessel function $K_0(x)$ and we arrive at the avalanche condition $\lambda = 1$ as

$$1 = \frac{m g_{\mathrm{ep}}^2}{\omega_0 E} K_0\left(\frac{2\Gamma\sqrt{2m\omega_0}}{E}\right), \tag{11}$$

which is one of our main results.

We turn our attention to the integral, Eq. (10), which is quite revealing. In the $E = 0$ limit, the s integral gives $\delta(q^2/2m + \omega_0) = 0$ due to the absence of target electronic states below the band edge, as depicted in Fig. 1(a). Therefore, in the equilibrium limit, there is no enhancement for an avalanche. At a finite E, the pole at $qs = -2im\Gamma/E$ results in a dominant contribution while smearing the energy conservation due to the time-dependent Hamiltonian and leads to a strong enhancement for an avalanche.

Using the asymptotic relation of $K_0(x)$ for large x, we can express the solution in the small avalanche field E_{av} limit as (see Appendix B for details)

$$E_{\mathrm{av}} \approx \frac{2\Gamma\sqrt{2m\omega_0}}{\ln\left(\sqrt{\frac{\pi}{32}}\beta\right)}, \tag{12}$$

with the avalanche parameter defined as

$$\beta = \frac{g_{\mathrm{ep}}^2}{\Gamma} \left(\frac{2m}{\omega_0^3}\right)^{1/2}. \tag{13}$$

III. DISCUSSIONS

In the following, we will compare the avalanche condition (11) against numerical results. Two of the most fundamental aspects of the quantum avalanche are displayed in Fig. 3. In

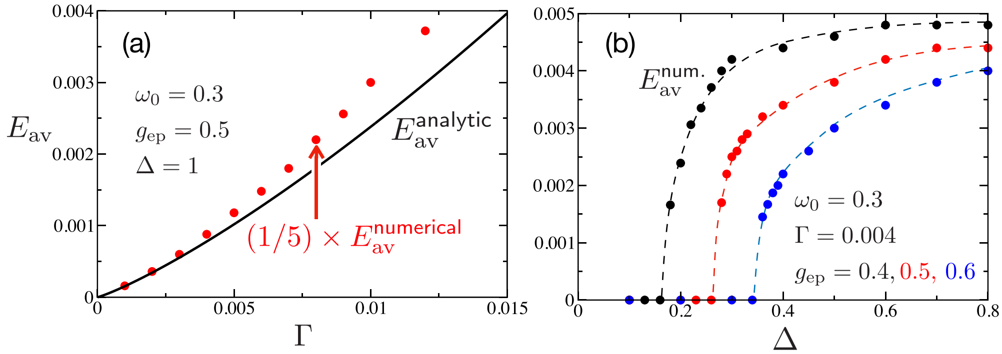

FIG. 3. (a) Avalanche field E_{av} versus dephasing rate Γ, numerical (data points), and analytic (solid line) results. $E_{av} \to 0$ as $\Gamma \to 0$ almost linearly. (b) Saturation of E_{av} with large Δ. The saturation shows that the avalanche is due to the fundamental instability of the conduction band itself, not due to the proximity to the particle reservoir. The initial absence of E_{av} at small Δ is due to the shift of gap by the electron-phonon coupling. The dashed lines are a guide to the eye.

(a), almost linear dependence between E_{av} and Γ illustrates the fact that the $\Gamma = 0$ limit is fundamentally singular in the nonequilibrium limit [16] and that the dephasing is crucial in understanding nonequilibrium steady state. Throughout the comparison to numerical results, there is an overall factor 5 discrepancy in E_{av}. While it might have been due to overestimating the renormalization factor λ in Eq. (11), the match between the analytical and numerical results is quite good apart from the overall factor. In Appendix A we discuss possible sources for the discrepancy.

The saturation of E_{av} for large Δ in Fig. 3(b) is quite surprising. The weak dependence of E_{av} on large Δ suggests that the avalanche is not a function of the proximity of the band to the particle source, but rather a fundamental instability of the conduction band itself once the particle source is accessible. This observation is consistent with Fig. 1(c), in which the avalanche occurred earlier with lower initial occupations in the band. In the analytic argument, it is a quite natural conclusion since Eq. (11) is a result of integration between fermion GFs where the energy difference enters and the gap Δ dependence drops out. The following discussions resulting from Eq. (11) correspond to the large Δ limit. We caution here that E_{av} saturates only with the model parameter Δ and, in physical systems, the gap dependence could come back indirectly since the band gap is roughly proportional to the phonon energy [30].

The dependence on the phonon parameters ω_0 and g_{ep} are shown in Figs. 4(a) and 4(b). The monotonic dependence is expected since a larger phonon energy requires a stronger E field. It is still remarkable that the curvature change agrees between the analytic and numerical results. The coupling constant dependence in (b) is impressive. The inverse dependence is expected since a weak coupling requires a higher field to generate an avalanche. What is interesting is that the sharp increase occurs at a finite value of g_{ep}.

The threshold behavior of g_{ep} can be understood analytically. As shown in Fig. 4(c), the right-hand side (RHS) of Eq. (11) is a nonmonotonic function. As g_{ep} decreases the maximum of the RHS hits 1, after which there does not exist an avalanche solution anymore. By parametrizing $x = 2\Gamma\sqrt{2m\omega_0}/E$, this condition amounts to $[xK_0(x)]'_{x=x_0} = 0$ at $x_0 = 0.595047$. Equation (11) can be rewritten as $xK_0(x) = 4/\beta$ with Eq. (13). Therefore, the critical condition for the existence of an avalanche becomes

$$\left.\frac{g_{ep}^2}{\Gamma}\left(\frac{2m}{\omega_0^3}\right)^{1/2}\right|_c = \frac{4}{x_0 K_0(x_0)} = 8.574 = \beta_c, \tag{14}$$

demonstrating the competition between the dephasing and the avalanching mechanism.

Numerical solutions predict peculiar reentrant behaviors near the threshold. As shown in Fig. 4(d), E_{av} values increase as g_{ep} is reduced. The n_{ex} curves after the avalanche do not simply collapse to zero as g_{ep} is reduced, but they develop reentrant avalanche domes before they reach $\beta = \beta_c$. We speculate that the electrons get excited after an avalanche and the additional dephasing due to charge fluctuations mitigates the avalanche, leading to the dome behavior. We emphasize that this most elementary nonequilibrium interacting model presents us with rich physics. The inclusion of the phonon self-energy did not change the reentrant behavior.

The competition between the avalanching mechanism and the dephasing is best summarized in the g_{ep}-Γ phase diagram for the existence of an avalanche [see Fig. 5(a)]. According to Eq. (14), the line $\beta = \beta_c$ (or $g_{ep} \propto \sqrt{\Gamma}$) divides the phase with avalanche ($\beta > \beta_c$) and that without avalanche ($\beta < \beta_c$). The numerical results deviate from the analytic theory at large $\Gamma(\gtrsim 0.005)$ due to the additional dephasing from the excitation of phonons. A related mechanism is discussed below.

Finally, we discuss the temperature dependence of the avalanche in Fig. 5(b). In the resistive switching literature, the conventional understanding based on the thermal scenario is that the switching field of the insulator-to-metal transition, mostly in Mott insulators, decreases with increasing temperature since the order in solids softens with temperature [31]. The quantum avalanche [16] mechanism, however, predicts the opposite trend which agrees with the soft and low-field resistive transitions observed in prototype charge-density-wave systems [1]. This is due to the thermal dephasing counteracting the avalanching mechanism. Therefore, understanding the numerical temperature dependence of E_{av} is crucial. As shown in (b), the temperature T^* at which the E_{av} changes significantly is at $T^* \approx 0.17\omega_0$. At this temperature, the Bose-Einstein function $n_b(\omega_0) = (e^{\omega_0/T^*} - 1)^{-1}$ is less than 0.005, which suggests that the mechanism may not be straightforward.

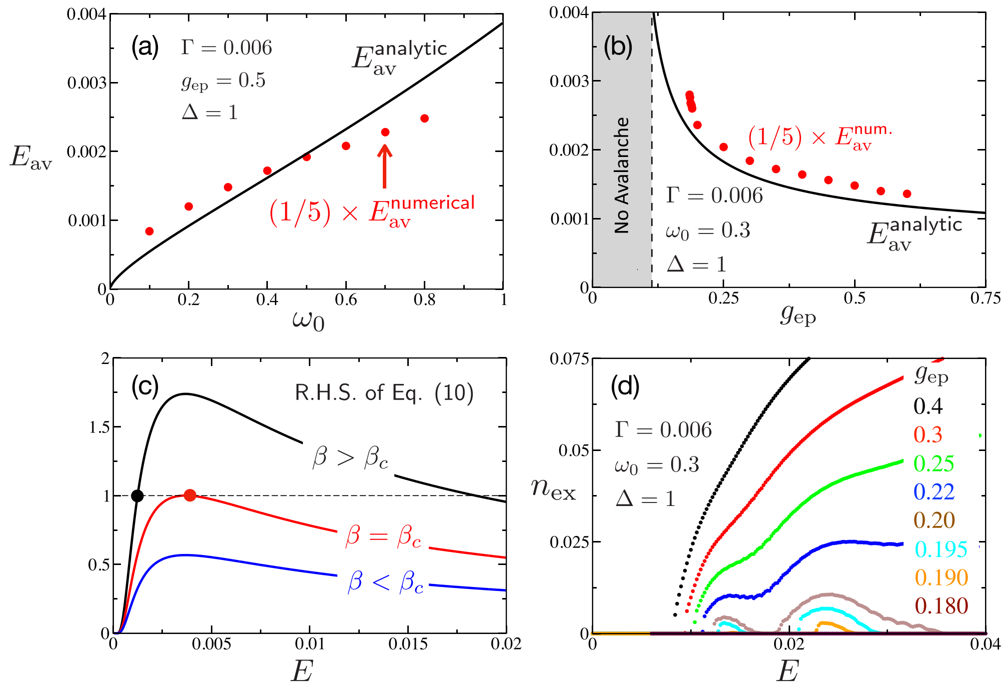

FIG. 4. (a) Avalanche field $E_{\rm av}$ versus phonon frequency ω_0. The electron replica generation is inversely proportional to ω_0, thus needing a larger E field to generate high phonon energy. (b) $E_{\rm av}$ versus electron-phonon coupling $g_{\rm ep}$. Not only the inverse dependence on $g_{\rm ep}$ but also the sharp increase at a threshold $g_{\rm ep}$ is well agreed between the numerical and analytic results. (c) Graphs for criterion Eq. (11), as $g_{\rm ep}$ is varied. Solutions (dots) cease to exist for $\beta < \beta_c$. (d) Numerical results of $n_{\rm ex}$ vs E field as $g_{\rm ep}$ is varied. As $g_{\rm ep}$ approaches the threshold value, the avalanche becomes reentrant with the size of domes eventually diminishing to zero at the threshold $g_{\rm ep}$.

The numerical temperature dependence is resolved by introducing the additional dephasing due to the electron-phonon coupling. The dephasing is evaluated from the retarded self-energy $\Sigma^R(\omega)$ at the band edge $\omega = \Delta$. Since the $\Sigma^>$ contribution dominates Σ^R, we have in the small E-field limit (see Appendix C for details)

$$-{\rm Im}\,\Sigma^R(\Delta) \approx \frac{m g_{\rm ep}^2}{2\omega_0\sqrt{2m\omega_0}} n_b(\omega_0) = \frac{1}{4}\Gamma\beta n_b(\omega_0). \quad (15)$$

By replacing Γ in Eq. (11) by the effective dephasing $\Gamma + |{\rm Im}\,\Sigma^R(\Delta)|$, we define the activation temperature T^* at $|{\rm Im}\,\Sigma^R(\Delta)| \approx \frac{1}{4}\Gamma$ and obtain

$$T^* = \frac{\omega_0}{\ln(1+\beta)}. \quad (16)$$

The position for T^*, marked by arrows in Fig. 5(b), agrees well with the numerical results.

IV. CONCLUSION

In conclusion, we proposed avalanche instability as a fundamental mechanism for a nonequilibrium quantum criticality. Analytical theory, with comprehensive agreement with numerical calculations, demonstrates the quantum origin of

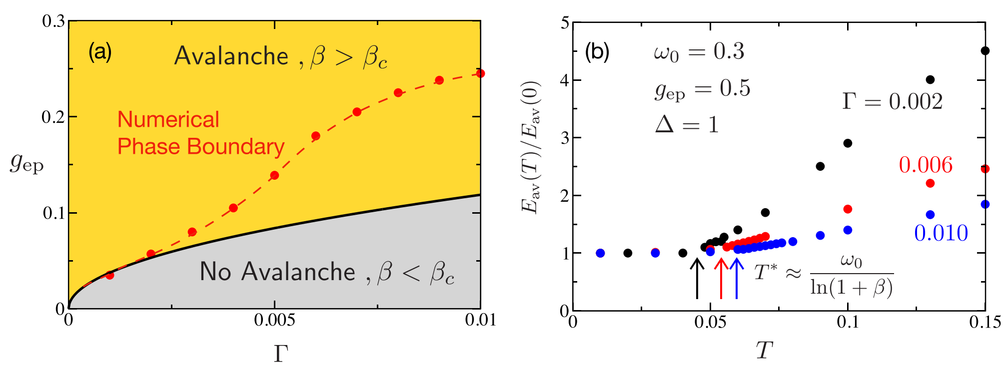

FIG. 5. (a) Γ-$g_{\rm ep}$ phase diagram for avalanche. The competition between the electron-phonon coupling and the dephasing results in the phase boundary line $\beta = \beta_c$ ($g_{\rm ep} \propto \sqrt{\Gamma}$). $\beta > \beta_c$ supports the avalanche phase. $\Delta = 1$ and $\omega_0 = 0.3$. (b) Finite temperature behavior of $E_{\rm av}$. The increasing $E_{\rm av}(T)$ behavior is a direct evidence of a nonthermal mechanism. The analytic prediction of the temperature T^* at the onset (arrows) agrees well with the numerical $E_{\rm av}(T)$.

the avalanche as a building block for understanding dc nonequilibrium phases of electrons. Further studies are necessary to test the ubiquity of the mechanism under dephasing mechanisms in various interacting models. The dissipation medium of the model can be easily extended to different types such as photons with the light-matter coupling enhanced in quantum cavities.

ACKNOWLEDGMENTS

The authors acknowledge the computational support from the CCR at the University at Buffalo. J.E.H. benefited greatly from discussions with C. Aron for his insightful comments and encouragement and with K.-S. Kim who pointed out the importance of the multiphonon diagrams. Helpful discussions with E. Arrigoni, G. Kotliar, J. Bird, and P. Zhang are appreciated. J.E.H. is grateful for the hospitality of the ENS-CNRS where part of the work was completed.

APPENDIX A: CALCULATION DETAILS FOR THE FOURTH-ORDER SELF-ENERGY $\Sigma^{(4)}(t)$

The fourth-order self-energy $\Sigma^{(4)}(t_2, t_1)$, in the low-density limit, is approximated as

$$-i\frac{g_{\rm ep}^4}{(2\omega_0)^2}\int_{-\infty}^{\infty}\frac{dq}{2\pi}\int_{-\infty}^{\infty}\frac{dq'}{2\pi}\int_{t_1}^{-\infty}ds_1\int_{-\infty}^{t_2}ds_2 n_<(q')$$
$$\times e^{-\Gamma(t_2-s_2+t_1-s_1+|s_2-s_1|)}e^{i\omega_0(s_2-s_1+t_2-t_1)}$$
$$\times U_q(t_2,s_2)U_{q'}(s_2,s_1)U_q(s_1,t_1). \tag{A1}$$

After substitution $s_1 \to t_1 + s_1$ and $s_2 \to s_2 + t_2$, and then by changing the variables to the average variable $S = \frac{1}{2}(s_1 + s_2)$ and the relative variable $s = s_2 - s_1$, we have the integral as

$$i\frac{g_{\rm ep}^4}{(2\omega_0)^2}e^{-i[(\Delta-2\omega_0)t+E^2t^3/24m]}$$
$$\times\int\frac{dq}{2\pi}\int\frac{dq'}{2\pi}\int_{-\infty}^{\infty}ds\int_{-\infty}^{-|s|/2}dSn_<(q')e^{\Gamma(2S-|s+t|)+i\omega_0 s}$$
$$\times e^{\frac{i}{2m}(q+ET)^2s-\frac{i}{2m}(q'+ET)^2(t+s)-\frac{i}{m}(q-q')E(t+s)S}, \tag{A2}$$

where we used the transformation of integral

$$\int_{-\infty}^{0}ds_1\int_{-\infty}^{0}ds_2=\int_{-\infty}^{\infty}ds\int_{-\infty}^{-|s|/2}dS. \tag{A3}$$

As discussed in the main text, we replace $q + ET$ and $q' + ET$ by the gauge-independent q and q', respectively, and set $q' \approx 0$ due to the factor $n_<(q')$. Then after performing the integral over S, we have

$$-\frac{mn_{\rm ex}g_{\rm ep}^4}{(2\omega_0)^2}e^{-i[(\Delta-2\omega_0)t+E^2t^3/24m]}$$
$$\times\int\frac{dq}{2\pi}\int ds\frac{e^{-\Gamma(|s|+|s+t|)+i\omega_0 s}}{qE(t+s)+2im\Gamma}e^{i\frac{q^2s}{2m}+i\frac{q}{2m}E(t+s)|s|}. \tag{A4}$$

To further simplify the expression, we make a crucial approximation based on the parameter regime that $\frac{q^2}{2m}+\omega_0 \gg \Gamma \sim E$. Due to this condition, the convergence of the integral is controlled by the fast oscillation in $e^{i(\frac{q^2}{2m}+i\omega_0)s}$. Therefore, the exponential factors $e^{-\Gamma(|s|+|s+t|)}$ and $e^{i\frac{q}{2m}E(t+s)|s|}$ are slowly varying and the approximation $s \approx 0$ can be used. The fourth-order self-energy then becomes a function of only the relative time t as

$$\Sigma_p^{(4),<}(t)\approx-\frac{mn_{\rm ex}g_{\rm ep}^4}{(2\omega_0)^2}e^{-i[(\Delta-2\omega_0)t+E^2t^3/24m]}$$
$$\times\int\frac{dq}{2\pi}\int ds\frac{e^{i(q^2/2m+\omega_0)s}}{qE(t+s)+2im\Gamma}. \tag{A5}$$

See the discussion in the following paragraph for further justification. The enhancement factor λ evaluated at $t = 0$ is then

$$\lambda=\frac{\Sigma_p^{(4),<}(0)}{\Sigma_p^{(2),<}(0)}\approx\frac{img_{\rm ep}^2}{2\omega_0}\int\frac{dq}{2\pi}\int ds\frac{e^{i(q^2/2m+\omega_0)s}}{qEs+2im\Gamma}$$
$$=\frac{mg_{\rm ep}^2}{4\omega_0 E}\int_{-\infty}^{\infty}\frac{dq}{|q|}\exp\left(-\frac{2m\Gamma}{E}\frac{q^2/2m+\omega_0}{|q|}\right)$$
$$=\frac{mg_{\rm ep}^2}{\omega_o E}K_0\left(\frac{2\Gamma\sqrt{2m\omega_0}}{E}\right), \tag{A6}$$

with the modified Bessel function $K_0(x)$. Note that the unspecified parameter $n_{\rm ex}$ cancels out. We identify the avalanche at $\lambda = 1$ and thus Eq. (8) in the main text. It is noted that, since the occupation spectra $G^<(\omega)$ is localized near $\omega = \Delta$ [16], its integral over ω [i.e., $\Sigma^<(t = 0)$] is a good indicator for the avalanche.

We test the approximation leading to Eq. (A5) by comparing it to the numerical evaluation of the integral that retains the phase $e^{iqEs|s|/2m}$ and the exponential damping factor by $e^{-2\Gamma|s|}$ at $t = 0$

$$\lambda'=\frac{img_{\rm ep}^2}{2\omega_0}\int\frac{dq}{2\pi}\int ds\frac{e^{-2\Gamma|s|+i(q^2/2m+\omega_0)s+iqEs|s|/2m}}{qEs+2im\Gamma}. \tag{A7}$$

Although the integral converges very slowly due to the extreme oscillation in the integrand, especially in the low E limit, the agreement in Fig. 6 shows that the analytic approximation is reliable in the regime of interest.

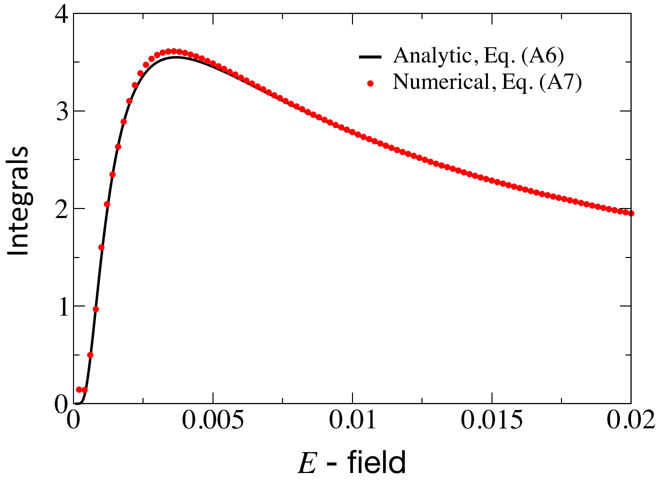

FIG. 6. Comparison of the numerical integral of Eq. (A7) (circles) as a function of E field against the analytic approximation Eq. (A6) (solid line) for typical parameters of $m = 1/2$, $\Gamma = 0.002$, $\omega_0 = 0.3$, and $g_{\rm ep} = 0.10$.

The result, Eq. (A6), is in excellent agreement with the numerical lattice calculations except for the overall magnitude difference of about factor 5 throughout. Since the two methods use different gauges, it is difficult to pinpoint the source of the discrepancy. However, the dispersion relation of the lattice model within the Brillouin zone $(-\pi,\pi)$ should be contrasted with the parabolic band of the continuum with the momentum in $(-\infty,\infty)$. If we limit the integral range of the second line of Eq. (A6) to $(-\pi,\pi)$, the integral should yield smaller results, which then should result in larger avalanche field values $E_{\rm av}$.

APPENDIX B: DERIVATION OF THE QUANTUM AVALANCHE FIELD, EQ. (12)

By using the parameter $x = 2\Gamma\sqrt{2m\omega_0}/E$ in Eq. (A6), we can express the avalanche condition as

$$xK_0(x) = \frac{4}{\beta} \quad \text{with } \beta = \frac{g_{\rm ep}^2}{\Gamma}\left(\frac{2m}{\omega_0^3}\right)^{1/2}, \tag{B1}$$

with the avalanche parameter β. In the large β limit, the solution to the criterion can be simplified by using the asymptotic relation of the Bessel function as

$$\left(\frac{\pi}{2}x\right)^{1/2} e^{-x} \approx \frac{4}{\beta}, \quad x \approx \ln\left(\sqrt{\frac{\pi}{32}}\beta\right) + \frac{1}{2}\ln x, \tag{B2}$$

which can be recursively solved as

$$x \approx \ln\left(\sqrt{\frac{\pi}{32}}\beta\right) + \frac{1}{2}\ln\left[\ln\left(\sqrt{\frac{\pi}{32}}\beta\right)\right] + \cdots. \tag{B3}$$

With the first term, the approximate solution for $E_{\rm av}$ is

$$E_{\rm av} \approx \frac{2\Gamma\sqrt{2m\omega_0}}{\ln\left(\sqrt{\frac{\pi}{32}}\beta\right)}. \tag{B4}$$

APPENDIX C: DERIVATION OF THE KICKOFF TEMPERATURE T^* IN $E_{\rm av}$, EQ. (16)

Since the retarded self-energy has the main contribution from the greater GF, we compute the greater self-energy in the low-field limit as

$$\Sigma^>(t) = -\frac{ig_{\rm ep}^2}{2\omega_0}\int\frac{dp}{2\pi}e^{-i(\Delta+p^2/2m)t}[(1+n_b)e^{-i\omega_0 t} + n_b e^{i\omega_0 t}], \tag{C1}$$

with the expression inside the bracket due to the phonon propagator, Eq. (5). At the band edge $\omega = \Delta$, the term proportional to $(1+n_b)$ vanishes due to the energy conservation and we have the Fourier transformation

$$\begin{aligned}\Sigma^>(\omega=\Delta) &\approx -\frac{ig_{\rm ep}^2 n_b}{2\omega_0}\int dp\,\delta(\omega_0 - p^2/2m)\\ &= -\frac{img_{\rm ep}^2}{\omega_0\sqrt{2m\omega_0}}n_b = -i(\beta/2)\Gamma n_b\end{aligned} \tag{C2}$$

and $\mathrm{Im}\,\Sigma^R(\omega) \approx \frac{1}{2}\mathrm{Im}\,\Sigma^>(\omega)$. Therefore, the effective dephasing rate becomes

$$\Gamma_{\rm eff} = \Gamma\left(1 + \frac{\beta}{4}n_b\right). \tag{C3}$$

We define the activation temperature T^* at the initial rise of $E_{\rm av}$ and conveniently set for the condition $\beta n_b = 1$, which leads to

$$T^* = \frac{\omega_0}{\ln(1+\beta)}. \tag{C4}$$

[1] J. Bardeen, Phys. Today 43(12), 25 (1990).
[2] J. Bardeen, Phys. Rev. B 39, 3528 (1989).
[3] B. K. Ridley, Proc. Phys. Soc. 82, 954 (1963).
[4] R. E. Thorne, J. Phys. IV France 131, 89 (2005).
[5] E. Janod, J. Tranchant, B. Corraze, M. Querré, P. Stoliar, M. Rozenberg, T. Cren, D. Roditchev, V. T. Phuoc, M.-P. Besland, and L. Cario, Adv. Funct. Mater. 25, 6287 (2015).
[6] H. Aoki, N. Tsuji, M. Eckstein, M. Kollar, T. Oka, and P. Werner, Rev. Mod. Phys. 86, 779 (2014).
[7] N. P. Ong, J. W. Brill, J. C. Eckert, J. W. Savage, S. K. Khanna, and R. B. Somoano, Phys. Rev. Lett. 42, 811 (1979).
[8] G. Grüner, Rev. Mod. Phys. 60, 1129 (1988).
[9] A. Zimmers, L. Aigouy, M. Mortier, A. Sharoni, S. Wang, K. G. West, J. G. Ramirez, and I. K. Schuller, Phys. Rev. Lett. 110, 056601 (2013).
[10] J. Zhang, A. S. McLeod, Q. Han, X. Chen, H. A. Bechtel, Z. Yao, S. N. Gilbert Corder, T. Ciavatti, T. H. Tao, M. Aronson, G. L. Carr, M. C. Martin, C. Sow, S. Yonezawa, F. Nakamura, I. Terasaki, D. N. Basov, A. J. Millis, Y. Maeno, and M. Liu, Phys. Rev. X 9, 011032 (2019).
[11] C. Zener, Proc. R. Soc. A 137, 696 (1932).
[12] T. Oka, R. Arita, and H. Aoki, Phys. Rev. Lett. 91, 066406 (2003).
[13] N. Sugimoto, S. Onoda, and N. Nagaosa, Phys. Rev. B 78, 155104 (2008).
[14] M. Eckstein, T. Oka, and P. Werner, Phys. Rev. Lett. 105, 146404 (2010).
[15] J. E. Han, J. Li, C. Aron, and G. Kotliar, Phys. Rev. B 98, 035145 (2018).
[16] J. E. Han, C. Aron, X. Chen, I. Mansaray, J.-H. Han, K.-S. Kim, M. Randle, and J. P. Bird, Nat. Commun. 14, 2936 (2023).
[17] F. S. Khan, J. H. Davies, and J. W. Wilkins, Phys. Rev. B 36, 2578 (1987).
[18] A. F. Kemper, M. A. Sentef, B. Moritz, T. P. Devereaux, and J. K. Freericks, Ann. Phys. (NY) 529, 1600235 (2017).
[19] J. Nathawat, I. Mansaray, K. Sakanashi, N. Wada, M. D. Randle, S. Yin, K. He, N. Arabchigavkani, R. Dixit, B. Barut, M. Zhao, H. Ramamoorthy, R. Somphonsane, G.-H. Kim,

K. Watanabe, T. Taniguchi, N. Aoki, J. E. Han, and J. P. Bird, Nat. Commun. **14**, 1507 (2023).

[20] T. M. Mazzocchi, P. Gazzaneo, J. Lotze, and E. Arrigoni, Phys. Rev. B **106**, 125123 (2022).

[21] S. Zhang and G.-W. Chern, arXiv:2201.02194.

[22] U. Weiss, *Quantum Dissipative Systems* (World Scientific, London, 2008).

[23] J. Khurgin, Y. J. Ding, and D. Jena, Appl. Phys. Lett. **91**, 252104 (2007).

[24] L. V. Keldysh, J. Exptl. Theor. Phys. (U.S.S.R.) **34**, 1138 (1958) [Sov. Phys. JETP **7**, 788 (1958)].

[25] J. Li, C. Aron, G. Kotliar, and J. E. Han, Phys. Rev. Lett. **114**, 226403 (2015).

[26] J. Li and J. E. Han, Phys. Rev. B **97**, 205412 (2018).

[27] C. Aron, G. Kotliar, and C. Weber, Phys. Rev. Lett. **108**, 086401 (2012).

[28] S. Onoda, N. Sugimoto, and N. Nagaosa, Prog. Theor. Phys. **116**, 61 (2006).

[29] J. E. Han, Phys. Rev. B **87**, 085119 (2013).

[30] P. Y. Yu and M. Cardona, *Fundamentals of Semiconductors* (Springer, Berlin, 2010).

[31] K. Maki, Phys. Rev. B **33**, 2852 (1986).